SINERGI Vol. 26, No. 1, February 2022: 1-6
http://publikasi.mercubuana.ac.id/index.php/sinergi
http://doi.org/10.22441/sinergi.2022.1.001

Performance analysis of various types of surface crack detection based on image processing

Regina Lionnie[1], Rizky Citra Ramadhan[1], Ahmad Syadidu Rosyadi[1], Muzammil Jusoh[2], Mudrik Alaydrus[1]
[1]Department of Electrical Engineering, Faculty of Engineering, Universitas Mercu Buana, Indonesia
[2]Faculty of Engineering Technology, Universiti Malaysia Perlis, Malaysia

Abstract
Major cracks on a highway or bridge's concrete surface have a massive risk of damages, accompanied by less maintenance, slow detection, and handling; the worst case of the damage is the structure's total collapse, which can produce fatalities. Moreover, Indonesia's climate and geographical location contribute to a higher level of potential damage to the structure. In order to reduce the potential damage, the need for a surface crack detection system arises. This research analysed three different databases (Database A, B, and C) with different surface concrete crack types, such as early thermal contraction, plastic shrinkage, corrosion reinforcement, and non-crack images. The total images from each Database vary from 14 images for Database A, 80 images for Database B, and 4000 images for Database C. The Otsu thresholding and mathematical morphology operations such as opening, closing, dilation, and erosion with pre-processing methods were combined and produced results for each Database with classification using Euclidean distance calculation. The best results for Database A and B were 100% using combination Otsu thresholding with Laplacian operator and Laplacian of Gaussian filter and the same result for a combination of mathematical morphological operations. The best result using Database C, which had more images than Database A and B, was 80,2% using a combination of mathematical morphological operations.

Keywords:
Corrosion Crack Image;
Early Thermal Crack Image;
Mathematical Morphology;
Otsu Thresholding;
Plastic Shrinkage Crack Image;

Article History:
Received: February 21, 2021
Revised: June 27, 2021
Accepted: July 8, 2021
Published: February 1, 2022

Corresponding Author:
Regina Lionnie
Department of Electrical Engineering,
Universitas Mercu Buana,
Indonesia
Email:
regina.lionnie@mercubuana.ac.id

INTRODUCTION

To accelerate economic equality and minimize social inequality, under the leadership of our president, Ir. H. Joko Widodo, Indonesia employed the National Strategic Plan (Rencana Strategies Nasional). One plan from 245 strategic plans is to build transportation infrastructure of land, sea, and air. Building the highway of 5.000 km is one of the land infrastructures targets [1]. However, a highway or bridge has a considerable risk of damages, accompanied by less maintenance, slow detection, and handling; the worst case of the damage is the structure's total collapse, which can produce fatalities. If only the crack detection had been found and handled earlier, this accident would not have happened.

The crack of concrete structures such as highways and bridges consist of two types based on the width of the crack, and the first type is micro-crack because of shrinkage of the concrete material with the width of 1mm, and this shallow crack does not reduce the concrete strength. The second type is the major crack with more than 2mm width. This second type of crack has the potential for the collapse of structures [2]. Furthermore, Indonesia's climate with high rainfall and high humidity makes the potential of

the damage rise to a higher level. Furthermore, geographically, Indonesia was located on the ring of fire, which causes frequent earthquakes and contributes to the higher level of potential damage to the structures [3].

The researches attributed to the surface crack detection engage on various methods such as edge detection with Sobel and combination with Otsu thresholding [4], wavelet denoising and Laplace to pre-process the images [5], edge detection methods with spatial and frequency domain for autonomous inspection of the structures [6], Min-Max Gray Level Discrimination (M2GLD) as pre-processing method before thresholding with Otsu [7], edge-based crack width transform technique (CWT) in [8] and MorphLink-C method with the artificial neural network as a classifier [9]. Most research focused on detecting the crack surface, but this research focused on different surface concrete crack types such as early thermal contraction, plastic shrinkage, and corrosion reinforcement. By knowing the type of surface crack earlier can help the authorized party handle the damage further. This action can prevent the damage from developing further. This research measured the detection system's performance using mathematical morphology and Otsu thresholding with the combination of pre-processing methods based on several Databases of the surface crack with a different type of concrete surface crack.

MATERIAL AND METHOD

Types of Surface Crack

Crack is the broken on the concrete's surface shown as lines that can be categorized with three parameters: the width, the length, and the pattern [10]. Several types of surface crack such as plastic settlement, plastic shrinkage, early thermal contraction, long-term drying shrinkage, surface crazing, corrosion of reinforcement, alkali-silica reaction, longitudinal and transverse crack. This research analysed three types of cracks: early thermal contraction, plastic shrinkage, and corrosion reinforcement. Figure 1 shows examples of images with respected types of cracks, from top to bottom, early thermal contraction, plastic shrinkage, and corrosion reinforcement crack images.

- Early Thermal Contraction: Early thermal contraction occurs when there are differences in the temperature caused by the cementing process's heating and cooling effect.
- Plastic Shrinkage: This type of crack usually occurs after one until 8 hours of the concrete placement process when the concrete loses water because of air, temperature, and wind on the concrete surface.
- Corrosion Reinforcement: As the name suggests, this type of crack happened because of the steel bones' corrosion inside the concrete due to the chemical reaction with the environment. The corroded steel bones grow in volume three times the original and create a crack on the concrete.

Mathematical Morphology

Mathematical morphology is a tool to extract features from an image to be components that are useful to represent and descript the entire image. Examples of extracted features are boundaries, skeletons, and convex hulls. The basic operations in mathematical morphology are erosion, dilation, opening, and closing [11].

Operation of opening an image *I* with the structuring element *sI* is shown in (1). First, the image will be processed by erosion operation with *sI* and dilation operation with sl. Next, the closing operation of an image *I* is shown in (2). It is the opposite of the opening operation; while the opening first image is eroded then dilated, the closing operation will dilate the image first and then erode it with the structuring element *sI*. The erosion operation works by removing the part of an image smaller than the structure's size; if the part of an image is wider than the structuring element, it shrinks or thins the part of an image.

On the other hand, the dilation operation works by growing or thickening part of an image by the structuring element's size [12].

Figure 1. Examples of images with respected types of cracks, from top to bottom, early thermal contraction, plastic shrinkage, and corrosion reinforcement crack images

The erosion and dilation processes are shown respectively in (3) and (4). Equation (3) indicates that erosion of an image *I* by structuring element *sl* is the set of all points *z* such that *sl* is translated by *z* is contained in *I*. Equation (4) indicates that the set of all displacements *z* such that $(\widehat{sl})$ and *I* overlap by at least one element. *I* and *sl* are set in Z^2 [13].

$$I \circ sl = (I \ominus sl) \oplus sl \quad (1)$$

$$I \bullet sl = (I \oplus sl) \ominus sl \quad (2)$$

$$I \ominus sl = \{z|(sl)_z \subseteq I)\} \quad (3)$$

$$I \oplus sl = \left\{z|(\widehat{sl})_z \cap I \neq \emptyset)\right\} \quad (4)$$

Otsu Thresholding

The thresholding method by Otsu is a method that divides the histogram of an image into two different parts automatically by calculating the threshold value that maximizes the between-class variances and minimizes the weighted within-class variance [14]. The minimized weighted within-class variance can be seen in (5). The threshold value is *n* while the left side of the sum operation is the first class while the right side of the sum operation is the second class. Operation *m* in (6) indicates the mean intensity value within the respective class, *p* is the normalized histogram of the image, and *i* indicates pixels ranges between 0 and *I* with *n* shown the threshold pixel value [13]. Thus, the thresholding process will divide the image into two parts, i.e., foreground and background.

$$\sigma_w^2(n) = (\sum_{i=0}^{n} p_i \sum_{i=0}^{n}[i - m_1(n)]^2 \frac{p_i}{\sum_{i=0}^{n} p_i}) + (\sum_{i=n+1}^{I} p_i \sum_{i=n+1}^{I}[i - m_2(n)]^2 \frac{p_i}{\sum_{i=n+1}^{I} p_i}) \quad (5)$$

$$m_1(n) = \sum_{i=0}^{n} \frac{ip_i}{\sum_{i=0}^{n} p_i} \text{ and } m_2(n) = \sum_{i=n+1}^{I} \frac{ip_i}{\sum_{i=n+1}^{I} p_i} \quad (6)$$

Design Of Proposed System

The crack detection system based on image processing designed in this research is organized as follows, the input of the detection system was the digital images of crack surface. The image was then pre-processed by converting the color images into grayscale images and various combinations of pre-processing methods such as a smoothing filter of Gaussian filter and median filter, Laplacian operator Laplacian of Gaussian filter. Next, the input images were processed using Otsu thresholding or mathematical morphology operations. Finally, Euclidean distance nearest neighbour was applied to the system for classification. Nearest neighbour is a flexible technique and the simplest machine learning algorithm because it can classify test data into label classes by searching for train data which is relatively the same as test data [15].

Furthermore, although it is a simple algorithm, it still provides good performance results [16]. The output performance was the accuracy result (%) of how the system can accurately classify the input images based on respected classes. Figure 2 shows the flowchart of the designed system.

There were three types of Databases used in this research, two surface crack databases (database A and database B) from the authors and one surface crack database (database C) from [17][18]. Database A consists of 14 images with seven surface crack images from the building and seven images of non-crack. Database B consists of 80 images with four types of crack (classes), three types of cracks early thermal contraction, plastic shrinkage, corrosion reinforcement, and one class of non-crack. Each class has 20 images, so the total images for Database B are 80 images: 60 images of crack from 3 types and 20 images of non-crack. The total images from Database C are 4000 images with 2000 images of surface crack and 2000 images of non-crack. Both databases have color (RGB) images, and the size of each image in the databases is different. The size of images in Database A and B is 280x160 pixels. The size of images in Database C is 227x227 pixels. Figure 3 shows the example of each Database's images, upper images from Database A, middle images from Database B, and bottom images from Database C.

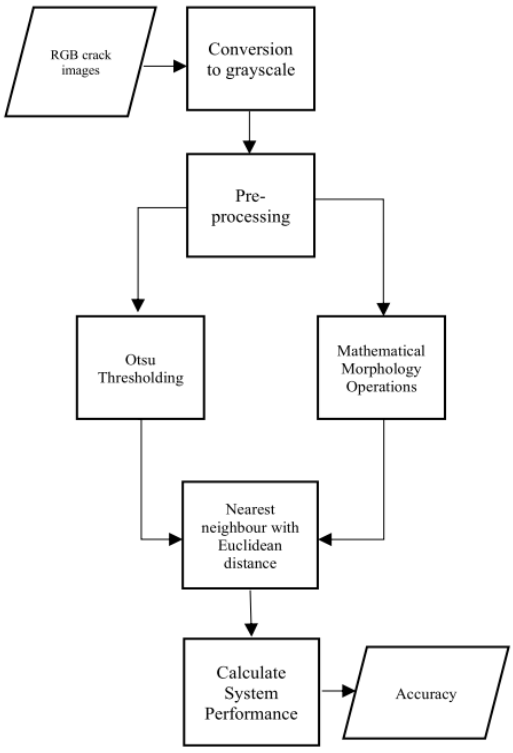

Figure 2. Flowchart of the designed system

Figure 3. Examples of images in the Database; Database A (top), Database B (middle), and Database C (bottom)

These various databases were analyzed using different types of classification. As mentioned before, the classifier used in this research was a simple Euclidean distance nearest neighbor. For Database A and Database B, the classifier's calculation is directly compared to the crack and non-crack images. For Database A, the classifier calculation used seven crack images and seven images of non-crack with one image as testing image and the rest 13 images of training images. For Database B, the classifier calculation used four images of crack from the same crack and four images of non-crack with one image as testing image and the rest seven images of training images. For Database C, due to many images, the system employed two-fold cross-validation as a statistical approach to help the system manage the images before the classification process. The images were scrambled first and then divided into two-fold training images, and testing images with each fold consisted of 2000 images of crack and non-crack images. After calculating the nearest distance, the system changed the training to be testing images and vice versa. Finally, the accuracy of the system was calculated in percentage. All simulations in this research were run using MATLAB 2016a and a computer with Intel Core i7—7500U CPU @ 2.70 and 2.90 GHz with 16Gb RAM.

RESULTS AND DISCUSSION

The results of this research are presented in Table 1, Table 2, and Table 3. Table 1 shows accuracy results from Database A, focusing on the Otsu thresholding method combined with several pre-processing methods such as smoothing filter with median and Gaussian, Laplace operator, Laplacian of Gaussian, and edge detection methods with Sobel and Prewitt.

Table 1. Results of Crack Detection System Using Database A

Method	Accuracy Result
Otsu Tresh + median filter	28%
Otsu Tresh + Gaussian filter	57%
Otsu Tresh + Laplacian	100%
Otsu Tresh + LoG	100%
Otsu Tresh + edge Sobel	85%
Otsu Tresh + edge Prewitt	85%

Table 2. Results of Crack Detection System Using Database B

Method	Accuracy Result
Mathematical Morph 1a	80%
Mathematical Morph 1b	95%
Mathematical Morph 1c	95%
Mathematical Morph 2a	100%
Mathematical Morph 2b	100%
Mathematical Morph 2c	100%

Table 3. Results of Crack Detection System Using Database C

Method	Accuracy Result
Otsu Tresh + median filter	79,03%
Otsu Tresh + Gaussian filter	78,80%
Otsu Tresh + Laplacian	50,03%
Otsu Tresh + LoG	50,15%
Otsu Tresh	78,38%
Mathematical Morph 1	54,35%
Mathematical Morph 2	55,70%
Mathematical Morph 3	80,2%
Without Otsu/MM	76,18%

Table 2 shows accurate results from Database B with focuses on Mathematical Morphology operations.

Mathematical Morph 1 indicates operations using closing from the input image, opening from closing, erosion from opening, removing inner pixels, and outlining and dilation from outlining process. The structuring element for closing, erosion, and dilation was line-shaped *sl* with distance from the center was 3, 3, and 2 respectively and 1800 counterclockwise for all operations. While structuring element for the opening was line-shaped *sl* with distance from the center was 18 and 950 counterclockwise. While Mathematical Morph 1a indicates Database B with images of plastic shrinkage surface crack, 1b with images with corrosion surface crack, and 1c with early thermal surface crack. Mathematical Morph 2 indicates operations using closing from the input image, opening from closing, erosion from opening, removing inner pixels, and outlining and dilation from outlining process. The structuring element for closing, erosion, and dilation was in line-shaped *sl* with distance from the center was 3, 2, and 2 respectively and with 1800 counterclockwise. While the structuring element for the opening was in line shaped with distance from the center was 18 and 950 counterclockwise.

Mathematical Morph 2a indicates Database B with images of plastic shrinkage surface crack, 2b with corrosion surface crack, and 2c with early thermal surface crack.

Table 3 shows accuracy results using Database C; all methods were applied to Database C because the Database consists of 4000 images with 2000 images of surface crack and 2000 images of non-surface crack [17-18]. Mathematical morphology operations 1 and 2 were the same as the previous explanation in Table 1 and Table 2, while operation 3 only consists of a combination of operations using closing from the input image, opening from closing, erosion from opening without removing inner pixels or outlining and without dilation. Other results are also added in Table 3 without using any method to test the classification results of distance calculation.

For Database, A results in Table 1, the method of Otsu thresholding was better if combined using the edge detection method of Sobel and Prewitt (85%), and the best results (100%) were produced by combining using Laplace operator and Laplacian of Gaussian (LoG). Otsu thresholding divided the grayscale pixels of an image into two parts. The filtering with Laplace operator and LoG also with edge detection method divided two parts in the Otsu thresholding classified between crack images and non-crack images better than filtering with smoothing process using median or Gaussian filter. Using the same method and combination but with a different database, Database C produced different results. Compared with the result without using any method (76,18%) in Table 3, applying Otsu thresholding gave slightly better results (78,38%), and the same better results if using smoothing filter of median and Gaussian (79,03% and 78,80% respectively). On the contrary, using the Laplace operator and LoG produced worse results for Database C (50,03% and 50,15%, respectively).

For Database B results in Table 2 with different types (classes) of surface crack, the mathematical morphological results produced 80% to 100%. The best results using Mathematical Morph 2 indicated operations using closing from the input image, opening from closing, erosion from opening, removing inner pixels, and outlining and dilation from the outlining process. The difference from operations 1 and 2 is located on the structuring element's length with line-shaped *sl* on the erosion process. The length of line-shaped *sl* on mathematical morph 1 was 3, while mathematical morph 2 was 2. Using the same method but with Database C, the accuracy results in Table 3 were lower (54,35% and 55,70%) compared to result without any method (76,18%). The mathematical morphology operations then changed into operation 3, which indicated a combination of operations using closing from the input image, opening from closing, erosion from opening without removing inner pixels or outlining, and without dilation in the end. The results of this combination of methods were the best, producing 80,2% of the accurate result. Different Databases produced varied results due to different types of crack and total images in the Database. This research was preliminary research due to a small number of images in certain databases (Database A and Database B).

CONCLUSION

The system of surface crack detection was built for this research. There were three types of Databases analyzed using Otsu Thresholding and mathematical morphological operations and their combination using pre-processing methods. The best results for Database A and B were 100% using combination Otsu thresholding with the Laplacian operator and LoG. The combination of mathematical morphological operations using closing from the input image, opening from closing, and erosion from opening, removing inner pixels and outlining and dilation from outlining process, respectively. The best result using Database C, which had more images compared to Database A and B, was 80,2% using mathematical morphological operations of closing from the input image, opening from closing, erosion from opening without removing inner pixels, or outlining, and without dilation. Further research needs to be performed with more images of surface cracks in the Database to improve the performance results.

ACKNOWLEDGMENT

This research was supported by Internal Research Grant of Research Center of Universitas Mercu Buana Jakarta No. 02-5/295/B-SPK/II/2021.

REFERENCES

[1] H. Kusuma, “Target Besar Jokowi RI Punya Jalan Tol 5.000 Km,” *DetikFinance*, Nov. 2019, [online] Available: https://finance.detik.com/infrastruktur/d-4774504/target-besar-jokowi-ri-punya-jalan-tol-5000-km [Accessed August 14, 2020].

[2] K. M. Nemati, P.J. Monteiro, and K.L. Scrivener, "Analysis of Compressive Stress-Induced Cracks in Concrete," *ACI Materials Journal*, vol. 95, no. 5, pp. 617-630, 1998, doi: 10.14359/404

[3] F. Ramdani, P. Setiani, D. A. Setiawati, “Analysis of sequence earthquake of Lombok Island, Indonesia,” *Progress in Disaster Science*, vol. 4, 100046, 2019, doi: 10.1016/j.pdisas.2019.100046
[4] A. M. A Talab et al., "Detection Crack in Image Using Otsu Method and Multiple Filtering in Image Processing Techniques," *Optik*, vol. 127, no. 3, pp. 1030-1033, 2016, doi: 10.1016/j.ijleo.2015.09.147
[5] H. Lei, J. Cheng, and Q. Xu, "Cement Pavement Surface Crack Detection Based on Image Processing," *Mechanical Engineering Science*, vol. 1, no.1, pp. 46-51, 2019, doi: 10.33142/me.v1i1.661
[6] S. Dorafshan., R. J. Thomas, R, and M. Maguire, "Benchmarking Image Processing Algorithms for Unmanned Aerial System-Assisted Crack Detection in Concrete Structures," *Infrastructures*, vol.4, no.2, pp. 1-16, 2019, doi: 10.3390/ infrastructures4020019
[7] N. D. Hoang, "Detection of Surface Crack in Building Structures Using Image Processing Technique with An Improved Otsu Method for Image Thresholding," *Advances in Civil Engineering*, vol. 2018, pp. 1-10, 2018, doi: 10.1155/2018/3924120
[8] H. Cho, H.J. Yoon, and J.Y. Jung. "Image-Based Crack Detection Using Crack Width Transform (CWT) Algorithm," *IEEE Access*, vol. 6, no. 1, pp. 60100-60114, 2018, doi: 10.1109/ACCESS.2018.2875889
[9] L. Wu, et al., "Improvement of Crack-Detection Accuracy Using a Novel Crack Defragmentation Technique in Image-Based Road Assessment," *Journal of Computing in Civil Engineering*, vol. 30, no. 1, pp. 04014118, 2016, doi: 10.1061/(ASCE)CP. 1943-5487.0000451
[10] G. Ramesh, D. Srinath, D. Ramya. B. V. Krishna, “Repair, rehabilitation and retrofitting of reinforced concrete structures by using non-destructive testing methods,” *Materials Today: Proceedings*, 2021, doi: 10.1016/j.matpr.2021.02.778.
[11] R. Kushol et al., "Contrast Enhancement by Top-Hat and Bottom-Hat Transform with Optimal Structuring Element: Application to Retinal Vessel Segmentation," *In Karray F. et al. (eds) ICIAR 2017*: *Image Analysis and Recognition Springer LNCS*, vol. 10317, pp 533-540, 2017, doi: 10.1007/978-3-319-59876-5_59
[12] R. Lionnie, F. E. Widyantoro, and M. Alaydrus, "A Study of Contrast Enhancement Methods in Various Color Spaces on Biometric Recognition System," *2019 Fourth International Conference on Informatics and Computing (ICIC)* Semarang Indonesia, pp. 1-4, 2019, doi: 10.1109/ICIC47613. 2019.8985866
[13] R. C. Gonzales, and R. E. Woods, *Digital Image Processing 3rd Edition*. New Jersey: Pearson Prentice Hall, 2008.
[14] A. Akagic, E. Buza, S. Omanovic, and A. Karabegovic, "Pavement Crack Detection Using Otsu Thresholding for Image Segmentation," *2018 41st International Convention on Information and Communication Technology, Electronics and Microelectronics (MIPRO)*, pp.1092-1097, 2018, doi: 10.23919/MIPRO.2018.8400199
[15] T. Wibowo and D. Fitrianah, "A K-Nearest Algorithm Based Application to Predict Snmptn Acceptance for High School Students in Indonesia," *International Research Journal of Computer Science*, vol 5, no. 1, pp. 9-20, 2018, doi: 10.26562/ IRJCS.2018.JACS10083
[16] A. Noor et al., "Melastoma Malabathricum L. Extracts-Based Indicator for Monitoring Shrimp Freshness Integrated with Classification Technology Using Nearest Neighbours Algorithm," *SINERGI*, vol. 25, no. 1, pp. 69-74, 2021, doi: 10.22441/sinergi. 2021.1.009
[17] C. F. Özgenel, A. Gönenç Sorguç, "Performance Comparison of Pretrained Convolutional Neural Networks on Crack Detection in Buildings," *2018 Proceedings of the 35th ISARC Berlin Germany*, pp. 693-700, 2018, doi: 10.22260/ISARC2018/0094
[18] L. Zhang, F. Yang, Y. D. Zhang, and Y. J. Zhu, "Road Crack Detection Using Deep Convolutional Neural Network," *2016 IEEE International Conference on Image Processing (ICIP)*, *Phoenix, AZ*, pp. 3708-3712, 2016, doi: 10.1109/ICIP.2016.7533052